Cancer Management and Research

Dovepress

open access to scientific and medical research

Open Access Full Text Article

ORIGINAL RESEARCH

Knockdown of hsa_circ_0000729 Inhibits the Tumorigenesis of Non-Small Cell Lung Cancer Through Mediation of miR-1281/FOXO3 Axis

Xiao Xie
Fangbao Ding
Haibo Xiao

Department of Cardiothoracic Surgery, Xinhua Hospital Affiliated to Shanghai Jiao Tong University School of Medicine, Shanghai, 200092, People's Republic of China

Background: Non-small cell lung cancer (NSCLC) is a subtype of lung cancer which seriously threatens the health of people. Circular RNAs (CircRNAs) are endogenous RNAs which have stable closed structure; they are known to be involved in tumorigenesis of NSCLC. Meanwhile, hsa_circ_0000729 was reported to be upregulated in NSCLC. Nevertheless, the function of hsa_circ_0000729 in NSCLC remains unclear.

Methods: Western blot and RT-qPCR were performed to investigate protein and mRNA levels, respectively. CCK-8 assay was performed to test the cell viability and cell death was investigated by flow cytometry. NSCLC cell pyroptosis was observed by electron microscope. In addition, the migration and invasion of NSCLC cells were detected by wound healing and transwell assay. The relation among hsa_circ_0000729, miR-1281 and FOXO3 was explored by dual-luciferase reporter assay and RNA pull-down.

Results: Hsa_circ_0000729 was found to be upregulated in NSCLC cells, and hsa_circ_0000729 knockdown obviously suppressed the proliferation of NSCLC cells through inducing pyroptosis. In addition, silencing of hsa_circ_0000729 notably inhibited the invasion and migration of NSCLC cells. Meanwhile, hsa_circ_0000729 could bind with miR-1281 and FOXO3 was directly targeted by miR-1281. Moreover, the anti-tumor effect of hsa_circ_0000729 siRNAs on NSCLC was markedly reversed by miR-1281 antagomir. Furthermore, silencing of hsa_circ_0000729 inhibited the tumor growth of NSCLC in vivo.

Conclusion: Knockdown of hsa_circ_0000729 inhibits the tumorigenesis of NSCLC through mediation of miR-1281/FOXO3 axis. Thus, hsa_circ_0000729 might be served as a crucial mediator in NSCLC.

Keywords: hsa_circ_0000729, miR-1281, FOXO3, pyroptosis

Introduction

Non-small cell lung cancer (NSCLC) is a type of lung malignant tumor. In addition, NSCLC is reported to be the leading cause of tumor-related mortality in the world.[1] Nowadays, the major treatments for NSCLC are radiotherapy, surgery and chemotherapy, while the prognosis of patients with NSCLC remains not ideal.[2,3] Although great studies have been made to treat NSCLC over 30 years, the survival rate of patients is still at low level due to the recurrence and metastasis of tumor.[4] Thereby, it is essential to explore new strategies against NSCLC.

Circular RNAs (CircRNAs) are endogenous RNAs which have stable closed structure.[5] It has been revealed that circRNAs participate in the cancer progression. For instance, Yi et al found that hsa_circ_0001806 overexpression could increase

Correspondence: Fangbao Ding; Haibo Xiao
Department of Cardiothoracic Surgery, Xinhua Hospital Affiliated to Shanghai Jiao Tong University School of Medicine, No. 1665 Kongjiang Road, Shanghai, 200092, People's Republic of China
Email dingfangbao@xinhuamed.com.cn; xiaohaibo@xinhuamed.com.cn

Received: 6 May 2021
Accepted: 12 September 2021
Published: 10 November 2021

the growth, migration and invasion of NSCLC cells via mediation of miR-1182/NOVA2 axis;[6] Wang et al indicated that circ-PTEN upregulation could suppress the proliferation of NSCLC cells through activation of PTEN.[7] Meanwhile, it has been revealed that hsa_circ_0000729 was significantly upregulated in lung adenocarcinoma (LUAD).[8] LUAD is the main subtype of NSCLC.[9] Nevertheless, the function of hsa_circ_0000729 in NSCLC remains largely unknown.

Recent studies indicated that pyroptosis plays a crucial role in cellular process.[10,11] Meanwhile, pyroptosis is a programmed cell death which is majorly regulated by caspase 1.[12,13] In addition, caspase 1 is often upregulated when the growth of NSCLC cells is inhibited, suggesting that the promotion of pyroptosis might be associated with the progression of NSCLC.[14] Therefore, it is necessary to investigate the correlation between hsa_circ_0000729 and pyroptosis in NSCLC cells with the purpose of exploring new effective strategies against NSCLC.

This study sought to investigate the function of hsa_circ_0000729 in NSCLC. We hope this research would shed new lights on exploring the new methods for the treatment of NSCLC.

Materials and Methods

Cell Culture

NSCLC cell lines (A549, NCI-H1650 and NCI-H1299) and human normal lung epithelial BEAS-2B cell line were purchased from Chinese Academy of Sciences (Shanghai, China). In addition, cells were maintained in RPMI-1640 medium (Thermo Fisher Scientific, Waltham, MA, USA) containing FBS (10%, Thermo Fisher Scientific) and penicillin (100 U/mL) in an incubator at 37°C.

Cell Transfection

NCI-H1299 or A549 cells (5×10^3) were transfected with hsa_circ_0000729 siRNA1 (si-hsa_circ_0000729-1), hsa_circ_0000729 siRNA2 (si-hsa_circ_0000729-2), hsa_circ_0000729 siRNA3 (si-hsa_circ_0000729-3) or negative control (NC; siRNA-ctrl) for 24 h by using Lipofectamine® 2000 (Invitrogen). Hsa_circ_0000729 siRNA1, siRNA2, siRNA3 and siRNA-ctrl were purchased from Genepharma (Shanghai, China). After 24 h of transfection, cells were harvested of use in the subsequent analysis.

For miR-1281 transfection, NSCLC cells were transfected with miR-1281 agomir, miR-1281 antagomir or NC by using Lipofectamine® 2000 (Thermo Fisher Scientific). MiR-1281 agomir, antagomir and NC were obtained from Genepharma. After 24 h of transfection, cells were harvested for use in the subsequent analysis.

For hsa_circ_0000729 overexpression, NCI-H1650 cells were transfected with pcDNA3.1 or pcDNA3.1-hsa_circ_0000729 for 24 h by using Lipofectamine® 2000 (Thermo Fisher Scientific). pcDNA3.1 and pcDNA3.1-hsa_circ_0000729 were obtained from Genepharma.

CCK-8 Assay

NSCLC cell viability in each group was evaluated using a CCK-8 assay kit (Beyotime, Shanghai, China). In brief, NCI-H1299, A549 or NCI-H1650 cells (5×10^3) were treated with NC or si-hsa_circ_0000729-3. After 24, 48 or 72 h of incubation, cells were treated with CCK-8 reagents (10 μL) for 2 h. The absorbance (450 nm) was measured by a microplate reader.

Annexin V/PI Staining

After 48 h of transfection, NSCLC cells were trypsinized, washed with phosphate buffered saline and resuspended in Annexin V Binding Buffer. Then, cells were stained with 5 μL Annexin V and 5 μL propidium (PI) in the dark for 15 min. Cells were analyzed by flow cytometer (BD Biosciences, Franklin Lake, NJ, USA). In addition, the data were analyzed using FACS (BD Biosciences) with FlowJo (v10.6.2; BD Biosciences).

Reverse Transcription-Quantitative PCR (RT-qPCR)

Total RNA was extracted from liver cancer cell lines using TRIzol reagent (TaKaRa, Tokyo, Japan) according to the manufacturer's protocol. First-strand cDNA was synthesized using the PrimeScript RT reagent Kit (Takara). After that, RT-qPCR was performed by using the SYBR premix Ex Taq II kit (ELK bioscience, Wuhan, China). Real-Time qPCRs were performed in triplicate. The protocol of amplification was as follows: 2 minutes at 94°C, followed by 35 cycles (30 s at 94°C and 45 s at 55°C). The following primer pairs were used for RT-qPCR: hsa-circ-0000729 forward, 5′-AAGTGAGCATGTGTGTGCAGG-3′ and reverse, 5′-TCCACCTGCTCACTTGCATG-3′; miR-1281 forward, 5′-TCGGTCGCCTCCTCCTC-3′ and reverse, 5′-CTCAACTGGTGTCGTGGAGTC-3′; β-actin forward, 5′-GTCCACCGCAAATGCTTCTA-3′ and

reverse, 5′-TGCTGTCACCTTCACCGTTC-3′; U6 forward, 5′-CTCGCTTCGGCAGCACAT-3′ and reverse, 5′-AACGCTTCACGAATTTGCGT-3′. The levels of gene were quantified using the $2^{-\Delta\Delta t}$ method. β-actin or U6 was used an internal reference.

Western Blot

Total protein was isolated from cell lysates or tissues by using RIPA buffer. The concentration of protein was detected with a BCA protein kit (Thermo Fisher Scientific). Then, proteins (40 μg per lane) were separated with 10% SDS-PAGE gel and then transferred into polyvinylidene fluoride (PVDF, Thermo Fisher Scientific) membranes. The PVDF membranes were incubated overnight with primary antibodies after being blocked with 3% skim milk for 1 h. The primary antibodies were as follows: anti-FOXO3 (1:1000), anti-cleaved caspase 1 (1:1000), anti-GSDME-N (1:1000) and anti-β-actin (1:1000). After that, the membrane was incubated with goat anti-rabbit secondary antibody (HRP-labeled, 1:5000) for 1 h. All antibodies were obtained from Abcam (Cambridge, MA, USA). ECL reagent (Thermo Fisher Scientific) was used to visualize the protein bands. ImageJ software (version 2.0) was performed to quantify the intensity of the

Transwell Assay

The upper chamber was pre-treated wi 50 μ matrig (This procedure was not included migrati assay) NSCLC cells (4×10^4) were sus nded DMEM (200 μL, Thermo Fisher Scientifi ithout FB The lower chamber was supplemented with c culture medium containing 20% FBS. Fo wing incub on for 24 h, the migrated or invade cells were fixed and stained with crystal violet (0.2) for min. The result was observed by a microsc e (mag ication 200).

Wou d He ng Assay

A549 cell e plated at a density of 2×10^5 cells per well. When A549 lls reached 80% confluence, a wound area was scratched in the cell monolayer using a pipette tip. After that, cells were treated with sihsa_circ_0000729-3 or sihsa_circ_0000729-3 + miR-1281 antagomir for 24 h at 37°C. Images were captured at 0 and 24 h under a fluorescence microscope (Leica Microsystems, Inc.).

ELISA

The levels of IL-18 and IL-1β in supernatants of NSCLC cells were investigated by ELISA detection kit (Multisciences (Lianke) Biotech Co., Ltd, Hangzhou, China) according to the manufacturer's instructions.

Dual-Luciferase Reporter Assay

The partial sequences of hsa_circ_0000729 and the FOXO3 3′-UTR containing the sites of miR-1281/miR-1178/miR-324-5p/miR-767-3p were synthesized by GenePharma. The aforementioned sequences were cloned into the pmirGLO vectors (Promega, Madison, WI, USA) for establishment of wild-type (WT) or mutant (MUT) reporter hsa_circ_0000729 and FOXO3 vectors. The WT or MUT hsa_circ_0000729 v ctor was ansfected into cells along with miR-128 iR-1178/mi 324-5p/miR-767-3p agomir using Lipofecta ine 200 reagent. The data were quantified by normalizing to enilla luciferase activity.

Scanning Electron Mi oscopy

NSCLC cells were fixed and rinsed three times. Su ently, cells were dehydrated through ethanol and ied by using the tertiary butanol method. After that, amples wer mounted and dried in a silica gel vacuum d iccator. nally, the morphology was observed by a sca g electron microscope (SEM, 20 kV).

RNA Pull-Down Assay

Probe-control or probe-hsa_circ_0000729 was transcribed and labeled with a Biotin RNA Labeling Mix (Roche, Basel, Switzerland). Cells were lysed with Poly-lysis buffer (ELK bioscience), washed with PBS and centrifuged at 1000 × g for 5 min at 4°C. Secondary structure formation in the biotin-labeled RNAs was induced with RNA structure buffer (Thermo Fisher Scientific). Streptavidin beads (75 μL; Thermo Fisher Scientific) were washed and incubated overnight. After that, streptavidin bead-RNA complexes were obtained by separating the mixture. Then, cell lysates (5×10^7 cells) were added to the complexes and incubated for 1 h. Following incubation, the mixture was separated again, and the supernatant of cell lysates was utilized to detect the enrichment of miR-1281. Meanwhile, RT-qPCR was performed to investigate the enrichment of miR-1281.

In vivo Study

BALB/c nude mice (n=8; 6–8 weeks old) were obtained from Vital River (Beijing, China). The protocols for animal care and use of laboratory animals were in accordance with ethical committee of Xinhua Hospital Affiliated to Shanghai Jiao

Tong University School of Medicine (No. XH20200725). A549 cells transfected with 50 nM si-hsa_circ_0000729-3 were subcutaneously transplanted in mice. The tumor volume was investigated once a week as the following formula: length × width × width. At end of the study, mice were sacrificed for tumor tissue collection. All in vivo experiments were performed according to the guideline of National Institutes of Health for the care and use of laboratory animals.

Statistical Analysis

Data were presented as the mean ± standard deviation. CCK8 assay was performed in quintuplicate. Flow cytometry, Western blot, RT-qPCR, luciferase activity test and ELISA were repeated in triplicate. The other experiments were performed three times. In addition, Student's *t*-test was used to compare the difference between two groups. One-way analysis of variance and Tukey's post hoc tests were used for comparisons between ≥3 groups. $P < 0.05$ was considered to indicate a statistically significant difference.

Results

Knockdown of hsa_circ_0000729 Inhibited the Proliferation of NSCLC Cells

The background information of hsa_circ_0000729 is presented in Figure 1A. To investigate the expression of hsa_circ_0000729 in NSCLC cell lines, RT-qPCR was performed. As indicated in Figure 1B, the level of hsa_circ_0000729 in NSCLC cells (A549, NCI-H1650 and NCI-H1299) was much higher than that in BEAS-2B cells. Since hsa_circ_0000729 expression was much higher in A549 and NCI-H1299 cells, these two cell lines were selected of use in the following experiments. Additionally, the level of hsa_circ_0000729 in NSCLC cells was markedly decreased by si-hsa_circ_0000729 siRNA1, siRNA2 or siRNA3 (Figure 1C and D). Meanwhile, A549 and NCI-H1299 were more susceptible to si-hsa_circ_0000729-3, compared with other two siRNAs. Thus, si-hsa_circ_0000729-3 was selected of use in the subsequent

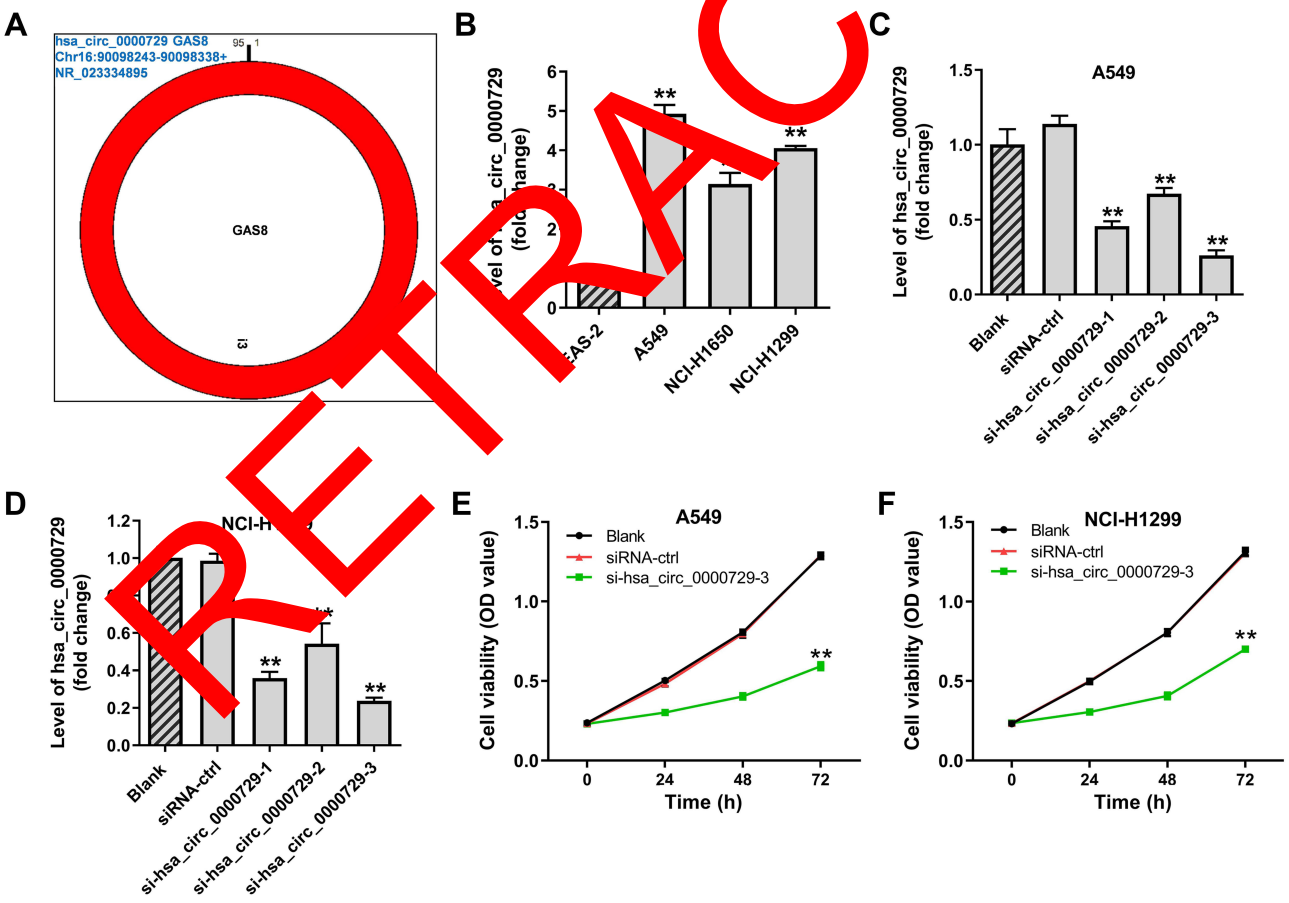

Figure 1 Knockdown of hsa_circ_0000729 inhibited the proliferation of NSCLC cells. (**A**) The background information of hsa_circ_0000729 was presented. (**B**) The expression of hsa_circ_0000729 in BEAS-2B, A549, NCI-H1650 or NCI-H1299 cells was detected by RT-qPCR. (**C** and **D**) A549 or NCI-H1299 cells were transfected with siRNA-ctrl (NC), hsa_circ_0000729 siRNA1, siRNA2 or siRNA3. Then, the expression of hsa_circ_0000729 in NSCLC cells was investigated by RT-qPCR. (**E** and **F**) NCI-H1299 cells were transfected with NC or si-hsa_circ_0000729-3. The viability of NSCLC cells was tested by CCK-8 assay. **P < 0.01 compared with control.

experiments. CCK8 data suggested si-hsa_circ_0000729-3 notably inhibited the viability of NSCLC cells (Figure 1E and F). Taken together, knockdown of hsa_circ_0000729 inhibited the proliferation of NSCLC cells.

Hsa_circ_0000729 siRNA Greatly Induced Pyroptosis in NSCLC Cells

In order to explore the manner of death in NSCLC cells, flow cytometry was used. As shown in Figure 2A–D, the percentage of cell death was significantly upregulated by hsa_circ_0000729 knockdown, and the ratio of PI positive cells was also notably increased by hsa_circ_0000729 siRNA3. The data suggested hsa_circ_0000729 knockdown might induce pyroptosis in NSCLC cells. Next, SEM was used to investigate if si-hsa_circ_0000729-3 could induce pyroptosis in NSCLC cells. The data revealed the membrane breakage and pyroptosis body in A549 or NCI-H1299 cells were significantly increased by si-hsa_circ_0000729-3 (Figure 2E and F). These phenomena were the typical feature of pyroptosis.[15] Thus, these data suggested that si-hsa_circ_0000729-3 greatly induced pyroptosis in NSCLC cells. Since A549 cells were more sensitive to si-hsa_circ_0000729-3 treatment (According to the result of CCK8, the inhibition rate of A549 cells after transfection of hsa_circ_0000729 siRNA3 was 54%, while the inhibition rate of NCI-H1299 cells was 46%), A549 cells were selected of... in the following experiments.

Hsa_circ_0000729 Could Bind with miR-1281

In order to explore the mechanism underlying the function of hsa_circ_0000729 in NSCLC tumorigenesis, the database (https://circinteractome.nia.nih.gov/) was used. The data revealed that hsa_circ_0000729 had a putative binding site with miR-1281 (Figure 3A). Also, miR-1178, miR-324-5p and miR-767-3p might be the downstream miRNAs of hsa_circ_0000729. In addition, the relative luciferase activity in WT-hsa_circ_0000729 was obviously inhibited by miR-1281 agomir, while miR-1281 agomir ... not affect the luciferase activity in MUT-hsa_circ_000...29 (Figure ...). Meanwhile, the luciferase activity in WT/M...T-hsa_circ_...0000729 was rarely affected by down-regulation of miR-...78, miR-324-5p or miR-767-3p (Supplementary Figure 1A–C). Next, the level of miR-1281 in NSCL... was significantly upregulated by miR-1281 ...omir but, ...ibited by miR-1281 antagomir (Figure 1C). In addition, the result of pulldown indicated the enrichment of miR-...281 was notably higher in probe-hsa_circ_0000729, compared with that in control (Figure 3D). Based on the above data, hsa_circ_0000729 possibly bind with miR-12...

... explore the potential target of miR-1281 ... Targetscan (http://www.targetscan.org/vert_72/) online tool and the database suggested miR-1281 had binding sites with FOXO3 (Figure 3E). Additionally, the

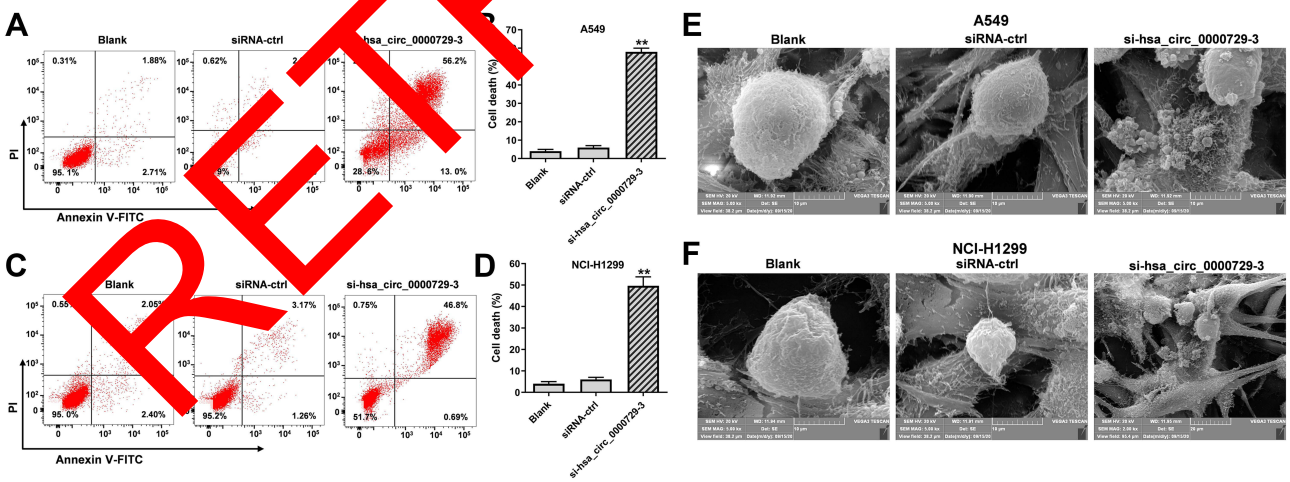

Figure 2 Si-hsa_circ_0000729-3 greatly induced pyroptosis in NSCLC cells. (**A** and **B**) The percentage of A549 cell death was tested by flow cytometry. (**C** and **D**) The percentage of NCI-H1299 cell death was tested by flow cytometry. (**E** and **F**) The pyroptosis of NSCLC cells was observed by SEM. **P < 0.01 compared with control.

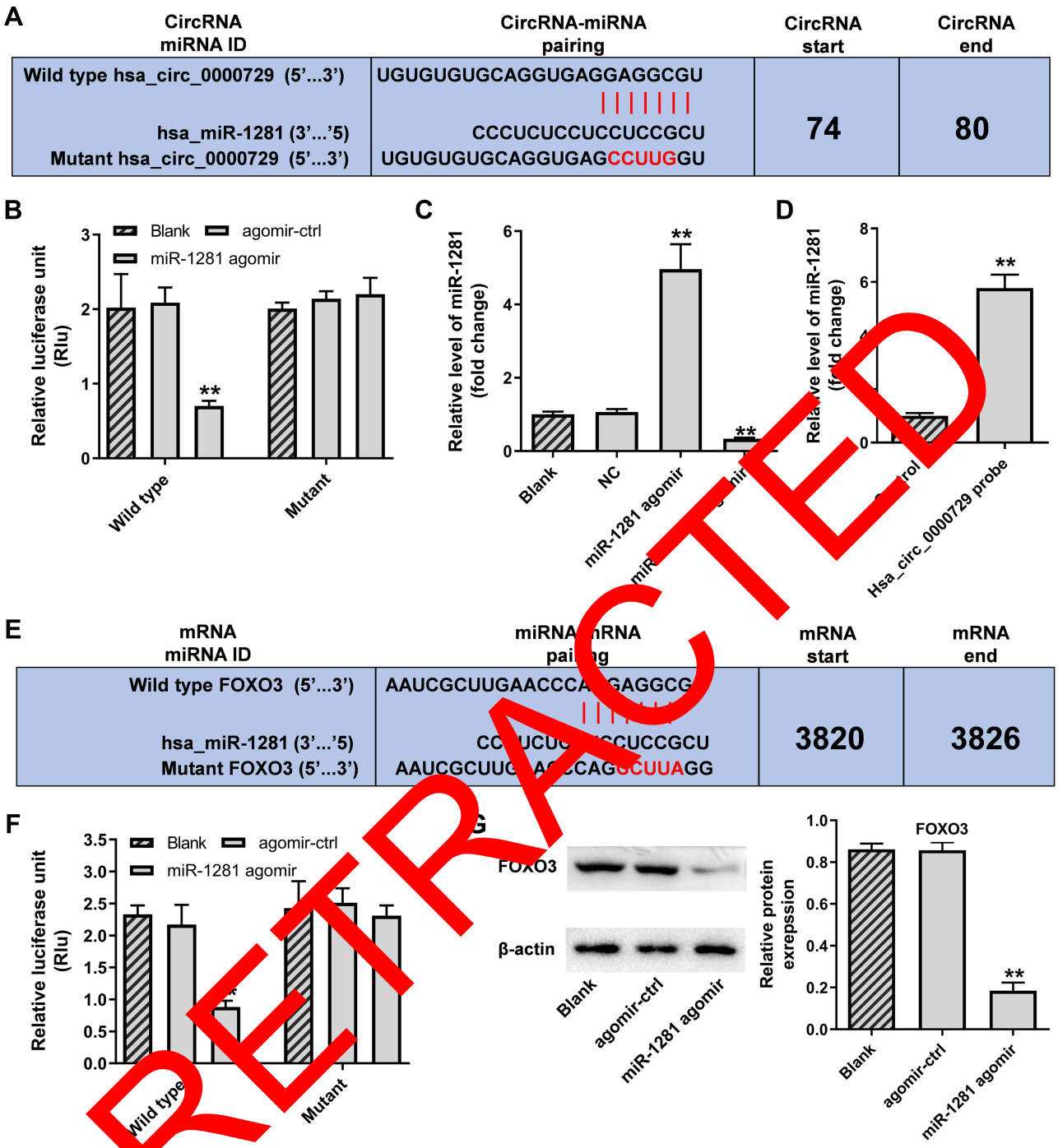

Figure 3 Hsa_circ_0000729 could bind with miR-1281. (**A**) Circular RNA Interactome was used to predict the downstream miRNA of hsa_circ_0000729. (**B**) The relative luciferase activity in WT/MUT-hsa_circ_0000729 was tested by dual luciferase reporter assay. (**C**) NSCLC cells were transfected with NC, miR-1281 agomir or miR-1281 antagomir. Then, the efficiency of cell transfection was detected by RT-qPCR. (**D**) The enrichment of miR-1281 was investigated by RNA pull-down. (**E**) FOXO3 was identified to be the direct target of miR-1281 by using targetscan online tool. (**F**) The relative luciferase activity in WT/MUT-FOXO3 was tested by dual luciferase reporter assay. (**G**) The protein level of FOXO3 in NSCLC cells was detected by Western blot. The relative expression was quantified by normalizing to β-actin. **P < 0.01 compared with control.

relative luciferase activity in WT-FOXO3 was significantly reduced in the presence of miR-1281 agomir (Figure 3F), and the protein level of FOXO3 in NSCLC cells was markedly decreased by miR-1281 agomir (Figure 3G). In summary, miR-1281 could bind with FOXO3.

Hsa_circ_0000729 Knockdown-Induced Pyroptosis in NSCLC Cells Was Significantly Reversed by miR-1281 Antagomir

To explore the mechanism by which hsa_circ_0000729 induced pyroptosis in NSCLC cells, Western blot was used. As demonstrated in Figure 4A–D, hsa_circ_0000729 siRNA significantly decreased the protein level of FOXO3 and upregulated the levels of cleaved caspase 1 and GSDME-N in NSCLC cells, while these phenomena were partially reversed by miR-1281 antagomir. In addition, hsa_circ_0000729 silencing-induced upregulation of IL-1β and IL-18 was notably abolished by miR-1281 antagomir (Figure 4E and F). Furthermore, miR-1281 antagomir partially reversed hsa_circ_0000729 knockdown-induced cell growth inhibition of NSCLC (Figure 4G–I). Since cleaved caspase 1, GSDME-N and IL-18 were known to be key mediators in pyroptosis,[16,17] it could be suggested that hsa_circ_0000729 knockdown-induced pyroptosis in NSCLC cells was through sponging miR-1281.

Silencing of Hsa_circ_0000729 Inhibited the Migration and Invasion of NSCLC Cells Through Sponging miR-1281

In order to further confirm the relation between hsa_circ_0000729 and miR-1281 in NSCLC, transwell and wound healing assay were performed. As shown in Figure 5A–C, the migration and invasion of NSCLC cells were notably inhibited by si-hsa_circ_0000729-3, while this phenomenon was partially reversed by miR-1281 antagomir. Therefore, these results indicated that silencing of hsa_circ_0000729 inhibited the migration and invasion of NSCLC cells through sponging miR-1281.

Overexpression of Hsa_circ_0000729 Increased the Viability, Migration and Invasion of NCI-H1650 Cells

To further confirm the function of hsa_circ_0000729 in NSCLC in vitro, NCI-H1650 cells were transfected with pcDNA3.1-hsa_circ_0000729. As revealed in Supplementary Figure 2A, the level of hsa_circ_0000729

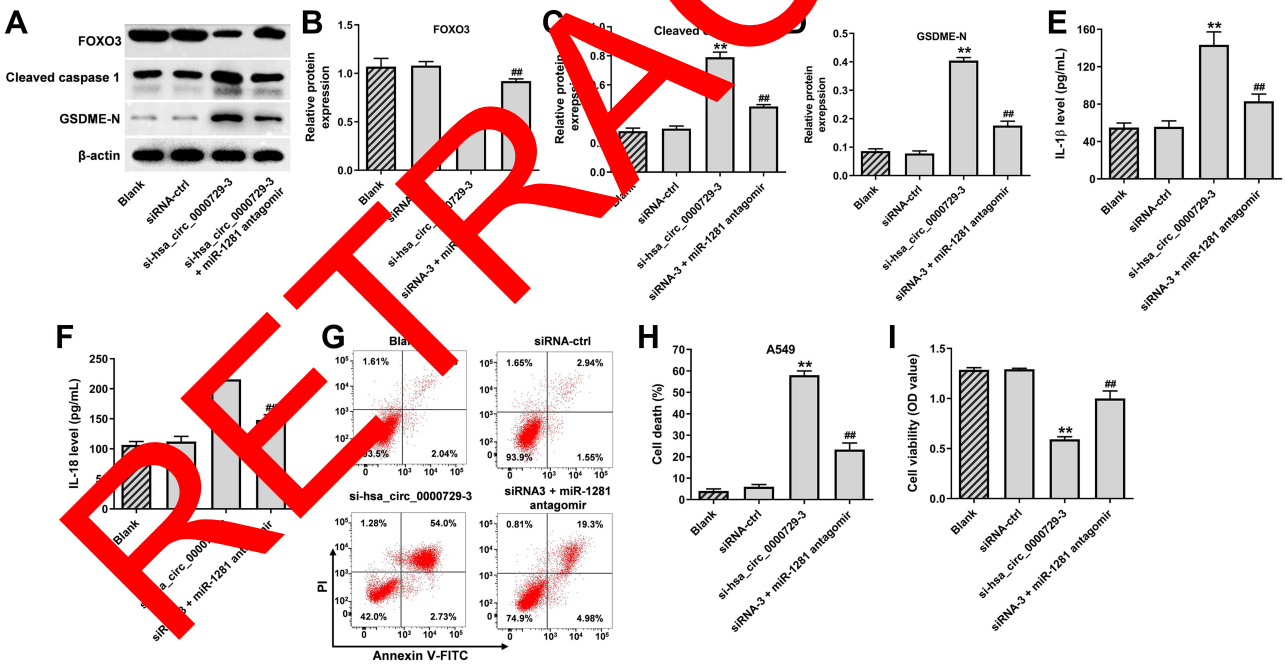

Figure 4 Hsa_circ_0000729 knockdown-induced pyroptosis in NSCLC cells was partially reversed by miR-1281 antagomir. NSCLC cells were treated with NC, si-hsa_circ_0000729-3 or si-hsa_circ_0000729-3 + miR-1281 antagomir. Then, (**A**) the protein levels of FOXO3, cleaved caspase 1 and GSDME-N in NSCLC cells were investigated by Western blot. (**B**–**D**) The relative expressions were quantified by normalizing to β-actin. (**E** and **F**) The levels of IL-1β and IL-18 in supernatants of NSCLC cells were tested by ELISA. (**G** and **H**) The percentage of NSCLC cell death was tested by flow cytometry. (**I**) The viability of NSCLC cells was detected by CCK-8 assay. **P<0.01 compared with control. ##P < 0.01 compared with si-hsa_circ_0000729-3.

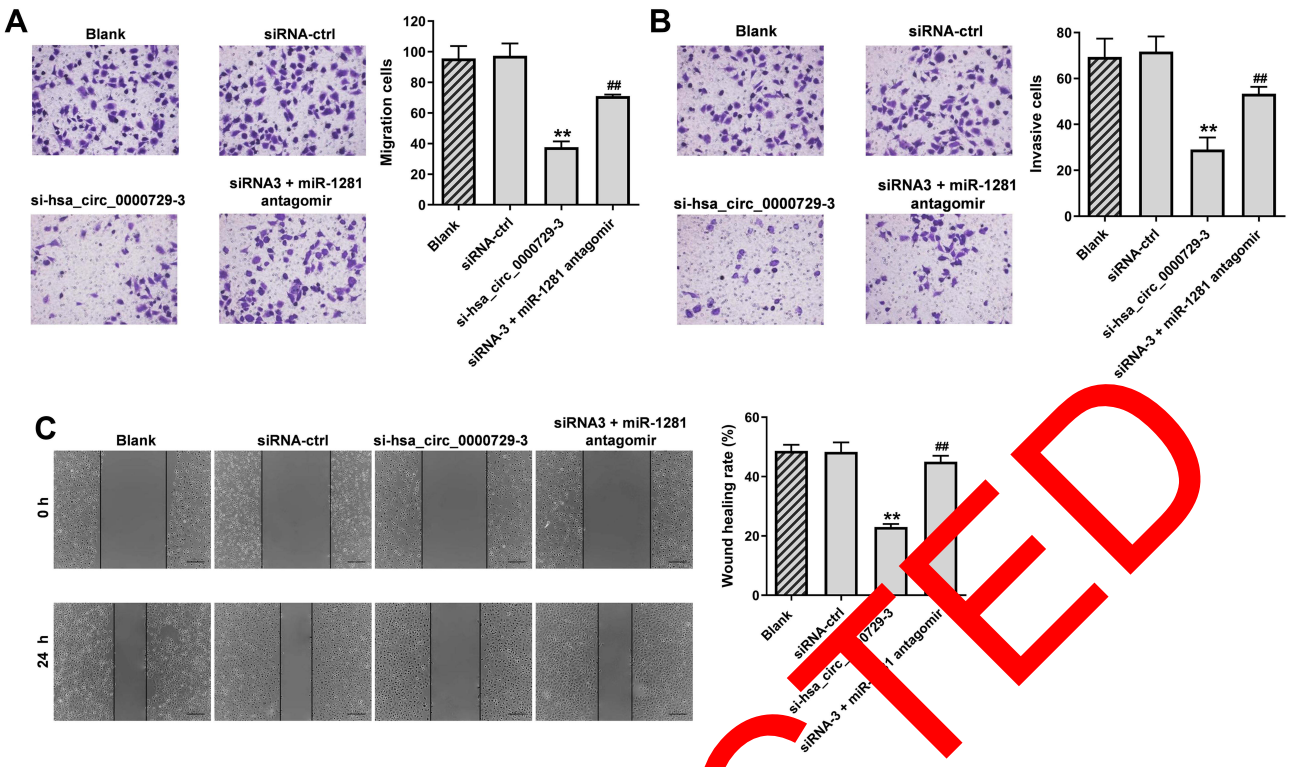

Figure 5 Silencing of hsa_circ_0000729 inhibited the migration and invasion of NSCLC cells through sponging miR-1281. (**A** and **B**) The migration and invasion of NSCLC cells were detected by transwell assay. (**C**) The migration of NSCLC cells was tested by wound healing assay. $^{**}P < 0.01$ compared with control. $^{\#\#}P < 0.01$ compared with si-hsa_circ_0000729-3.

in NCI-H1650 cells was significantly increased by pcDNA3.1-hsa_circ_0000729. In addition, hsa_circ_0000729 overexpression significantly increased the viability, migration and invasion of NCI-H1650 cells (Supplementary Figure 2B–D). In summary, overexpression of hsa_circ_0000729 increased the viability, migration and invasion of NCI-H1650 cells.

Hsa_circ_0000729 Knockdown Inhibited the Tumor Growth of NSCLC in vivo

To further investigate the function of hsa_circ_0000729 in NSCLC in vivo, a xenograft mice model was established. As revealed in Figure 6A and B, knockdown of hsa_circ_0000729 significantly decreased the tumor sizes in mice. Consistently, the tumor weight of mice was obviously decreased in the presence of si-hsa_circ_0000729-3 (Figure 6C). Meanwhile, hsa_circ_0000729 silencing markedly inhibited the expression of FOXO3 and upregulated cleaved caspase 1 and GSDME-N in tumor tissues of mice (Figure 6D–G). To sum up, hsa_circ_0000729 downregulation inhibited the tumor growth of NSCLC in vivo.

Discussion

It has been reported that circRNAs play vital roles in the progression of NSCLC.[18,19] In this research, hsa_circ_0000729 was found to be notably upregulated in NSCLC cells, and hsa_circ_0000729 knockdown could inhibit the progression of NSCLC. A previous research indicated that hsa_circ_0000729 could act as a potential prognostic biomarker in LUAD.[8] Our data was consistent to this previous research. In addition, the current study firstly explored the function of hsa_circ_0000729 in NSCLC, suggesting that hsa_circ_0000729 could act as a promoter in NSCLC.

It is reported that circRNAs could regulate the tumorigenesis of NSCLC through sponging miRNAs. For instance, Duan et al found that overexpression of hsa_circ_0074027 could lead to the development of NSCLC via mediation of miR-2467-3p;[20] Lu et al demonstrated that upregulation of hsa_circ_0020123 could facilitate the progression of NSCLC through binding with miR-142-3p.[21] In this study, miR-1281 could be bound with hsa_circ_0000729, firstly indicating the correlation between hsa_circ_0000729 and miR-1281 in NSCLC. In addition, miR-1281 has been reported to be the

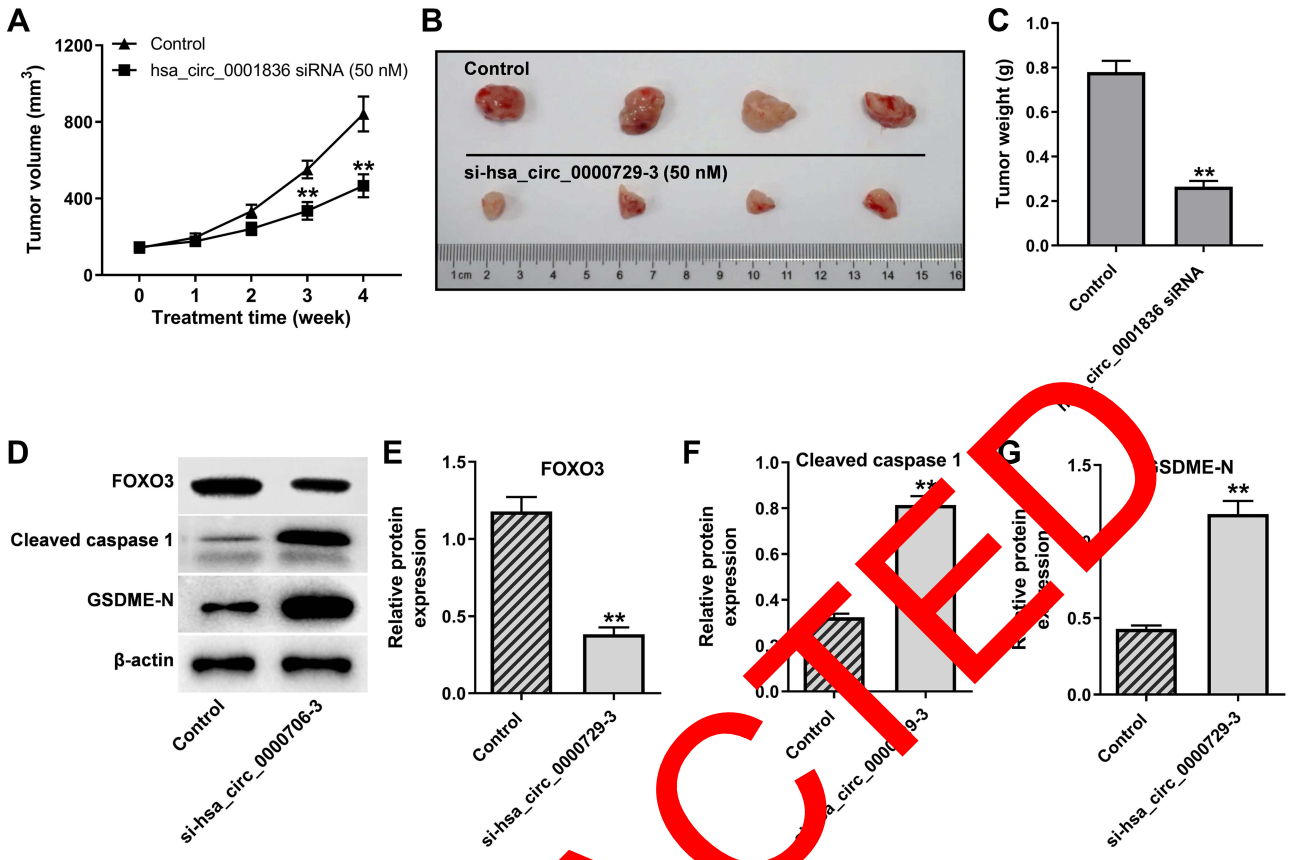

Figure 6 Hsa_circ_0000729 knockdown inhibited the tumor growth of N CLC i (**A**) The tumor volume of mice was tested weekly. (**B**) The tumor tissues of mice were pictured. (**C**) The tumor weight of mice was determined. (**D**) The pr in exp FOXO3, cleaved caspase 1 and GSDME-N in tumor tissues of mice were investigated by Western blot. (**E**–**G**) The relative expressions were quantifie rmalizing to β-actin. **P < 0.01 compared with control.

inhibitor in tumors.[22,23] Consistently, t study miR-1281 antagomir could reverse the ti-tum effect of hsa_circ_0000729 knockdown on CLC, which firstly suggested the function of miR-1281 in SCLC. Thus, it could be concluded that hs circ_0000729 ight regulate the tumorigenesis of N LC by ediation of miR-1281.

FOXO3 is known b key regulator in cell growth.[24] In our research O3 w identi d to be the direct target of miR-128 It has b en repor that FOXO3 participate in cell pyroptos [25] ould be suggested that hsa_circ_0000729 knockdown could induce pyroptosis in NSCLC cells w indirectly targeting FOXO3. Meanwhile, Hu et al found that miR-1281 inhibitor could reverse LNC01857 silencing-induced inhibition of glioma cell proliferation through upregulation of TRIM65.[26] Our data were similar to this previous study. TRIM65 was known to be a promoter in the progression of cancer. Consistently, FOXO3 is known to promote the cell growth.[27,28] Thereby, the similar function between FOXO3 and TRIM65 in cancer progression might result in the similarity between our study and Hu et al.

Caspase 1 and GSDME-N are known to be the important modulator in cell pyroptosis.[29,30] Activation of caspase 1 could lead to the upregulation of GSDME-N.[31,32] Meanwhile, IL-1β and IL-18 are also pyroptosis-related cytokines.[33,34] Consistently, our study revealed that knockdown of hsa_circ_0000729 could induce pyroptosis in NSCLC cells via upregulating cleaved caspase 1, GSDME-N, IL-1β and IL-18.

Indeed, there are some limitations in this research as follows: 1) more miRNAs sponged by hsa_circ_0000729 remain unclear; 2) more mRNAs targeted by miR-1281 in NSCLC cells are needed to be further explored. Thereby, more investigations remain to be performed in future.

In summary, knockdown of hsa_circ_0000729 inhibits the tumorigenesis of NSCLC through mediation of miR-1281/FOXO3 axis. Thus, hsa_circ_0000729 might be served as a crucial mediator in NSCLC.

Acknowledgements

This study was supported by the National Natural Science Foundation of China(Nos. 82173382).

Disclosure

These authors declare no competing interests in this research.

References

1. Xing JJ, Hou JG, Ma ZN, et al. Ginsenoside Rb3 provides protective effects against cisplatin-induced nephrotoxicity via regulation of AMPK-/mTOR-mediated autophagy and inhibition of apoptosis in vitro and in vivo. *Cell Prolif*. 2019;52(4):e12627. doi:10.1111/cpr.12627
2. Wen Q, Jiao X, Kuang F, et al. FoxO3a inhibiting expression of EPS8 to prevent progression of NSCLC: a new negative loop of EGFR signaling. *EBioMedicine*. 2019;40:198–209. doi:10.1016/j.ebiom.2019.01.053
3. Zhang Y, Zhao H, Zhang L. Identification of the tumorsuppressive function of circular RNA FOXO3 in nonsmall cell lung cancer through sponging miR155. *Mol Med Rep*. 2018;17(6):7692–7700.
4. Chen G, Yu L, Dong H, Liu Z, Sun Y. MiR-182 enhances radioresistance in non-small cell lung cancer cells by regulating FOXO3. *Clin Exp Pharmacol Physiol*. 2019;46(2):137–143. doi:10.1111/1440-1681.13041
5. Zhu Y, Zhao P, Sun L, et al. Overexpression of circRNA SNRK targets miR-103-3p to reduce apoptosis and promote cardiac repair through GSK3beta/beta-catenin pathway in rats with myocardial infarction. *Cell Death Discov*. 2021;7(1):84. doi:10.1038/s41420-021-00467-3
6. Yi S, Li Z, Wang X, Du T, Chu X. Circ_0001806 promotes the proliferation, migration and invasion of NSCLC cells through miR-1182/NOVA2 axis. *Cancer Manag Res*. 2021;13:3067–3077. doi:10.2147/CMAR.S290059
7. Wang Y, Wang Z, Lu J, Zhang H. Circular RNA circ-PTEN elevates PTEN inhibiting the proliferation of non-small cell lung cancer cells. *Hum Cell*. 2021;34(4):1174–84.
8. Li S, Sun X, Miao S, et al. hsa_circ_0[illegible]729, a potential prognostic biomarker in lung adenocarcinoma. *Thorac Cancer*. 2018;9(8):924–930. doi:10.1111/1759-7714.12761
9. Zhu J, Ao H, Liu M, Cao K, Ma J. UBE2T promotes autophagy via the p53/AMPK/mTOR signaling pathway in lung adenocarcinoma. *J Transl Med*. 2021;19(1):374. doi:10.1186/s12967-021-03056-1
10. Tan Y, Sun R, Liu L, et al. Tumor suppressor DRD2 facilitates M1 macrophages and restricts NF-kappaB signaling to trigger pyroptosis in breast cancer. *Theranostics*. 2021;11(11):5214–5231. doi:10.7150/thno.58322
11. Uematsu T, Suchiya K, Nishi N, et al. Mint3 depletion-mediated glycolytic and mitochondrial alterations promote pyroptosis and prevent the spread of Listeria monocytogenes infection in macrophages. *Cell Death Dis*. 2021;12(4):404. doi:10.1038/s41419-021-03691-y
12. Faria SS, Costantini S, de Lima VCC, et al. NLRP3 inflammasome-mediated cytokine production and pyroptosis cell death in breast cancer. *J Biomed Sci*. 2021;28(1):26. doi:10.1186/s12929-021-00724-8
13. Sok SPM, Ori D, Wada A, et al. 1′-acetoxychavicol acetate inhibits NLRP3-dependent inflammasome activation via mitochondrial ROS suppression. *Int Immunol*. 2021;33(7):373–386. doi:10.1093/intimm/dxab016
14. Peng Z, Wang P, Song W, et al. GSDME enhances Cisplatin sensitivity to regress non-small cell lung carcinoma by mediating pyroptosis to trigger antitumor immunocyte infiltration. *Signal Transduct Target Ther*. 2020;5(1):159. doi:10.1038/s41392-020-00274-9
15. Chen S, Zhou C, Yu H, et al. 27-Hydroxycholesterol contributes to lysosomal membrane permeabilization-mediated pyroptosis in co-cultured SH-SY5Y cells and C6 cells. *Front Mol Neurosci*. 2019;12:14. doi:10.3389/fnmol.2019.00014
16. Liu H, Zhang Y, Song W, Sun Y, Jiang Y. Osteopontin N-terminal function in an abdominal aortic aneurysm from apolipoprotein E-deficient mice. *Front Cell Dev Biol*. 2021;9:681790. doi:10.3389/fcell.2021.681790
17. Sun W, Liu S, Huang X, Yuan R, Yu J. Cytokine storms and pyroptosis are primarily responsible for the rapid death of mice infected with pseudorabies virus. *R Soc Open Sci*. 2021;8(8):210296. doi:10.1098/rsos.210296
18. Yue Q, Xu Y, Deng X, et al. Circ-PITX1 promotes the progression of non-small cell lung cancer through regulating the miR-1248/CCND2 axis. *Onco Targets Ther*. 2021;14:1807–[illegible] doi:10.2147/OTT.S286820
19. Zhao Q, Zhao F, Liu C, Xu T, Sun K. LncRNA FOXD2-AS1 promotes cell proliferation and invasion of fibroblast-like synoviocytes by regulation of miR-3[illegible]3p/PIAS[illegible] pathway in rheumatoid arthritis. *Autoimmunity*. 2021;54(5):25[illegible]263. doi:10.1080/08916934.2021.1919879
20. Duan Z, Wei S, Liu Y, [illegible] 007[illegible]27 contributes to non-small cell lung cancer progression through positively modulating RHOA via sequestering [illegible]-2467-3p. *J Bioenerg Biomembr*. 2021;53(2):223–23[illegible] doi:[illegible]007/s10863-0[illegible]09876-6
21. Lu J, Ma X, Lin J, He P. Circ_0020123 increases ZFX expression to facilitate non-small cell lung cancer progression by sponging miR-142-3p. *Cancer Manag Res*. 2021;13:1687–1698. doi:10.2147/CMAR.S295595
22. Lin LY, Shi K, Xu D, et al. LncRNA GIHCG regulates microRNA-1281 and promotes malignant progression of breast cancer. *Eur Rev Med Pharmacol Sci*. 2019;23(24):10842–10850.
23. Liu G, Jiang Z, Qiao M, Wang F. Lnc-GIHCG promotes cell proliferation and migration in gastric cancer through miR- 1281 adsorption. *Mol Genet Genomic Med*. 2019;7(6):e711. doi:10.1002/mgg3.711
24. Bi C, Wang G. LINC00472 suppressed by ZEB1 regulates the miR-23a-3p/FOXO3/BID axis to inhibit the progression of pancreatic cancer. *J Cell Mol Med*. 2021;25(17):8312–8328. doi:10.1111/jcmm.16784
25. Liang C, Liu Y, Xu H, et al. Exosomes of human umbilical cord MSCs protect against hypoxia/reoxygenation-induced pyroptosis of cardiomyocytes via the miRNA-100-5p/FOXO3/NLRP3 pathway. *Front Bioeng Biotechnol*. 2020;8:615850. doi:10.3389/fbioe.2020.615850
26. Hu G, Liu N, Wang H, Wang Y, Guo Z. LncRNA LINC01857 promotes growth, migration, and invasion of glioma by modulating miR-1281/TRIM65 axis. *J Cell Physiol*. 2019;234(12):22009–22016. doi:10.1002/jcp.28763
27. Wu X, Chang SC, Jin J, Gu W, Li S. NLRP3 in fl ammasome mediates chronic intermittent hypoxia-induced renal injury implication of the microRNA-155/FOXO3a signaling pathway. *J Cell Physiol*. 2018;233(12):9404–9415. doi:10.1002/jcp.26784
28. Yin Y, Wang J, Zhao X, et al. Overexpressed FOXO3 improves inflammatory status in mice by affecting NLRP3-mediated cell coronation in necrotizing colitis mice. *Biomed Pharmacother*. 2020;125:109867. doi:10.1016/j.biopha.2020.109867
29. Kim N, Choi JG, Ju IG. et al. A novel nutritional mixture, MBN, prevents memory impairment via inhibiting NLRP3 inflammasome formation in 5xFAD transgenic mice. *Nutr Neurosci*. 2021;1–8. doi:10.1080/1028415X.2021.1913952
30. Lou Y, Miao J, Li F, Ding J, Wang L. Maternal smoking during pregnancy aggravated muscle phenotype in FHL1(-/y) offspring mice similar to congenital clubfoot through P2RX7-mediated pyroptosis. *Toxicol Lett*. 2021;345:54–60. doi:10.1016/j.toxlet.2021.04.014

31. Xia W, Li Y, Wu M, et al. Gasdermin E deficiency attenuates acute kidney injury by inhibiting pyroptosis and inflammation. *Cell Death Dis*. 2021;12(2):139. doi:10.1038/s41419-021-03431-2
32. Li Y, Yuan Y, Huang ZX, et al. GSDME-mediated pyroptosis promotes inflammation and fibrosis in obstructive nephropathy. *Cell Death Differ*. 2021;28:2333–2350.
33. Garcia-Bonilla L, Sciortino R, Shahanoor Z, et al. Role of microglial and endothelial CD36 in post-ischemic inflammasome activation and interleukin-1beta-induced endothelial activation. *Brain Behav Immun*. 2021;95:489–501. doi:10.1016/j.bbi.2021.04.010
34. Zeng Y, Yan Wang C, Xu J, Le Xu X. Overexpression of retinoid X receptor beta provides protection against oxidized low-density lipoprotein-induced inflammation via regulating PGC1alpha-dependent mitochondrial homeostasis in endothelial cells. *Biochem Pharmacol*. 2021;188:114559. doi:10.1016/j.bcp.2021.114559